APPLIED MICROBIAL AND CELL PHYSIOLOGY

# AI-2 analogs and antibiotics: a synergistic approach to reduce bacterial biofilms

Varnika Roy · Mariana T. Meyer ·
Jacqueline A. I. Smith · Sonja Gamby ·
Herman O. Sintim · Reza Ghodssi · William E. Bentley

**Abstract** Quorum sensing (QS), the process of autoinducer-mediated cell–cell signaling among bacteria, facilitates biofilm formation, virulence, and many other multicellular phenotypes. QS inhibitors are being investigated as antimicrobials because of their potential to reduce symptoms of infectious disease while slowing the emergence of resistant strains. Autoinducer-2 (AI-2) analogs have been shown to inhibit genotypic QS responses among many bacteria. We demonstrate for the first time, the ability of C1-alkyl AI-2 analog, isobutyl-DPD, to significantly inhibit the maturation of *Escherichia coli* biofilms grown in vitro. Using a novel microfluidic device that incorporates dynamic, real-time measurements of biofilm density, we also show that a combinatorial approach wherein isobutyl-DPD ((S)-4,5-dihydroxy-2,3-pentanedione) is used with the antibiotic gentamicin is quite effective in rendering near complete clearance of pre-existing *E. coli* biofilms. Similarly, another AI-2 analog, phenyl-DPD, also used in combination with near MIC levels of gentamicin, resulted in clearance of preformed *Pseudomonas aeruginosa* biofilms. Clearance of pre-existing biofilms has remained a significant health care challenge; these results warrant consideration of a new approach based on the combination of "quenching" QS signal transduction processes with traditional antibiotic treatment.

**Keywords** AI-2 · Biofilms · Quorum quenching · Quorum sensing

Varnika Roy and Mariana T. Meyer have contributed equally to this work.

V. Roy
Graduate Program in Molecular and Cell Biology,
University of Maryland,
College Park, MD 20742, USA

V. Roy · M. T. Meyer · R. Ghodssi · W. E. Bentley (✉)
Fischell Department of Bioengineering, University of Maryland,
2330 Kim Engineering Building,
College Park, MD 20742, USA
e-mail: bentley@umd.edu

M. T. Meyer · R. Ghodssi
Institute for Systems Research, University of Maryland,
College Park, MD 20742, USA

J. A. I. Smith · S. Gamby · H. O. Sintim
Department of Chemistry and Biochemistry,
University of Maryland,
College Park, MD 20742, USA

R. Ghodssi
Department of Electrical and Computer Engineering,
University of Maryland,
College Park, MD 20742, USA

## Introduction

Bacteria that attach to surfaces can encase themselves in a self-synthesized hydrated matrix of polysaccharides and proteins to form slimy layers or biofilms (Costerton et al. 1999). Biofilms mediate persistence and shield bacteria from hostile environments. These structured communities enable a multicellular existence distinct from planktonic forms (Stewart and Costerton 2001). Within biofilms, microchannels maintain flow of nutrients (de Beer et al. 1994), and cells in different regions can display different gene expression patterns (Davies et al. 1993). These and other attributes such as metabolic cooperativity have led to the comparison of biofilms with tissues of higher organisms (Costerton et al. 1995). Biofilms are of high clinical relevance,

as they exist in ~80 % of human infections (Romero et al. 2008). Pathogens in biofilms can exhibit antibiotic tolerance ~1,000 times higher than their planktonic counterparts (Olson et al. 2002). Antibiotic therapy, most effective against plank-tonic cells that slough off biofilms, is oftentimes unable to eradicate the biofilm itself (Stewart and Costerton 2001). Thus, biofilm infections typically become chronic, leading to continual administration of antibiotics, which, in turn, con-tributes to the clinical challenge of antibiotic resistance.

There are various hypotheses for antibiotic resistance with-in biofilms (Mah and O'Toole 2001). First, antibiotics that interact with the exopolysaccharide are prevented from pene-trating thick biofilm layers (Bose and Ghosh 2011; Kumon et al. 1994). Second, altered chemical environments within the biofilm, for example by accumulation of acidic waste products (Zhang and Bishop 1996), are hypothesized to interfere with antibiotic activity (Dunne 2002; Stewart and Costerton 2001). Third, differences in nutrient concentrations and anaerobic niches within the biofilms can lead to persister cells. Persister cells are cells which have entered a dormant, inactive stage that are often compared to spores and can persist even in prolonged exposure to elevated antibiotic concentrations. Un-der favorable conditions, persisters can revert to live cells and reseed biofilm formation (Keren et al. 2004; Lewis 2010).

The formation of complex microstructures within biofilms is regulated by the exchange of chemical signals, including bacterial autoinducers, between cells (Davies et al. 1998; Singh et al. 2000). Oftentimes, behaviors that are cued by these autoinducers become multicellular in nature, a charac-teristic of bacterial quorum sensing (QS). *Pseudomonas aer-uginosa*, an opportunistic pathogen that forms thick biofilms within the lungs of cystic fibrosis patients, uses QS extensive-ly to modulate both biofilm formation and maturation. It has been shown that *P. aeruginosa* deficient in producing QS autoinducer formed thinner biofilms that were more sensitive to detergents compared to wild-type biofilms (Davies et al. 1998). Also, *P. aeruginosa* autoinducers, acylated homoserine lactones (AHLs, also referred to as autoinducer family, AI-1), were found at significantly higher concentrations (632 μM) in biofilms as compared to planktonic cells (14 nM) of the same organism (Pan and Ren 2009). Importantly, it was recently shown that AI-1-targeted small molecule QS inhibitors (QSI) can assist antibiotics in the clearance of biofilms in vivo (Brackman et al. 2011; Christensen et al. 2012). These reports and others (Geske et al. 2005; Rasmussen and Givskov 2006a, b; Rogers et al. 2009) support the notion that targeting QS signaling within biofilms may form the basis for a new ap-proach to treating bacterial infectious disease.

The second class of autoinducer, AI-2, is referred to as "universal" as its synthase, LuxS, is found in more than 70 bacterial species (Sun et al. 2004). Oral bacteria such as *Streptococcus mutans* (Merritt et al. 2003; Wen and Burne 2004) and *Streptococcus gordonii* (Blehert et al. 2003;

McNab et al. 2003) that were *luxS* deficient showed aberrant biofilms in monoculture. Addition of AI-2 to *Escherichia coli* increased their biofilm mass 30-fold (Gonzalez Barrios et al. 2006). Absence of the putative AI-2 exporter, YdgG, enhanced signaling and resulted to biofilm thickness and biomass that were 7,000- and 574-fold greater than controls, respectively (Herzberg et al. 2006). *E. coli* strains lacking the AI-2 signaling regulators *lsrK* and *lsrR* formed significantly thinner biofilms with altered architecture (Li et al. 2007). These reports confirm that, in addition to AI-1 signaling, altered AI-2 signaling plays an important role in biofilm formation.

We suggest, therefore, that QS signal transduction pro-cesses constitute a vast trove of components and targets for developing new antimicrobials (Roy et al. 2011). Inhibiting biofilm formation and maturation could slow the develop-ment of antibiotic resistance (Anderson and O'Toole 2008). Given its prevalence among Eubacteria, a few groups have developed AI-2 analogs (Lowery et al. 2008, 2009; Roy et al. 2010; Smith et al. 2009) as quorum sensing inhibitors, although none have performed detailed studies investigating how these AI-2-based analogs affect various bacterial bio-films. C1-alkyl analogs of AI-2, including isobutyl-DPD, were shown to be potent broad species QS inhibitors in *E. coli*, *Salmonella typhimurium*, and *Vibrio harveyi* (Roy et al. 2010; Smith et al. 2009). Notably, as shown in Scheme 1, isobutyl-DPD is phosphorylated by LsrK and inhibits QS-related *lsr* expression. It is thought that unlike AI-2, which is phosphorylated and switches *lsr* expression "on" by remov-ing the repressor of the circuit LsrR, isobutyl-DPD switches *lsr* expression "off" by maintaining the LsrR repressor/DNA complex (Roy et al. 2010). Interestingly, AI-2 analog, phenyl-DPD, inhibits QS-related pyocyanin production in *P. aeruginosa* (Gamby et al. 2012). While this species employs AI-1 for communication and does not synthesize AI-2, gene expression in *P. aeruginosa* is regulated by extracellular AI-2 produced by surrounding microflora (Duan et al. 2003) (Scheme 1b). In this study, we use the AI-2 analogs isobutyl-DPD and phenyl-DPD to test whether these "quorum quenchers" alter biofilm formation, maturation, and removal among *E. coli* and *P. aeruginosa*, respectively.

To develop a more detailed understanding, we have cre-ated a microfluidic setting useful for rapid real-time analy-sis. That is, most biofilm studies are performed in large flow cells (Sternberg and Tolker-Nielsen 2006) or batch reactors, with reactor volumes on the order of milliliters and above. In order to limit needed quantities of small molecule effec-tors (phenyl-DPD and isobutyl-DPD) and perform these experiments in a high-throughput manner, we conducted biofilm studies in custom-fabricated microfluidic flow cells with a volume of ~1 μL (Fig. 1) and cross-sectional dimen-sions on the order of hundreds of microns. Our device enables minimal reactant volumes, high throughput, and tight control over the microenvironment for cell culture. We operate several
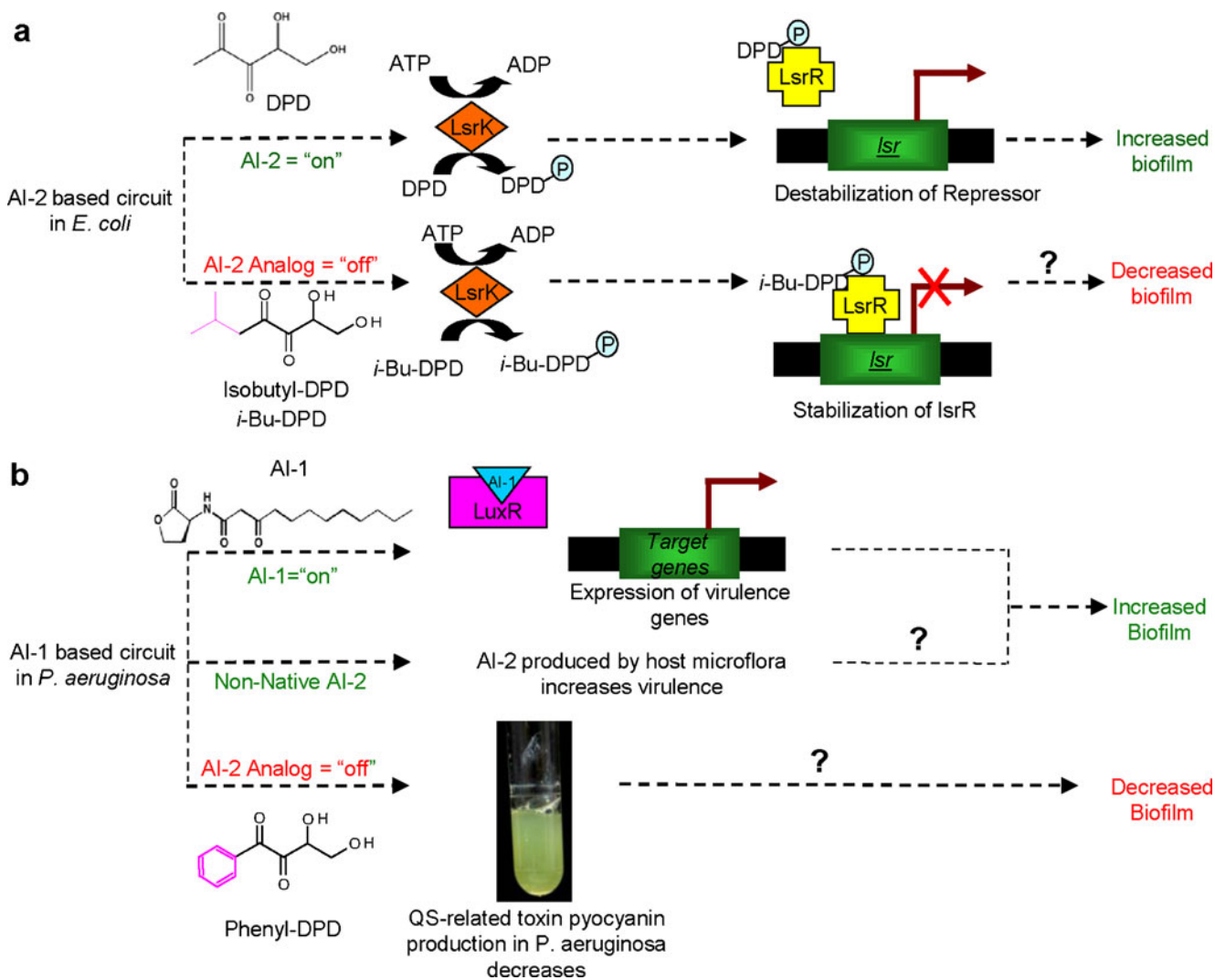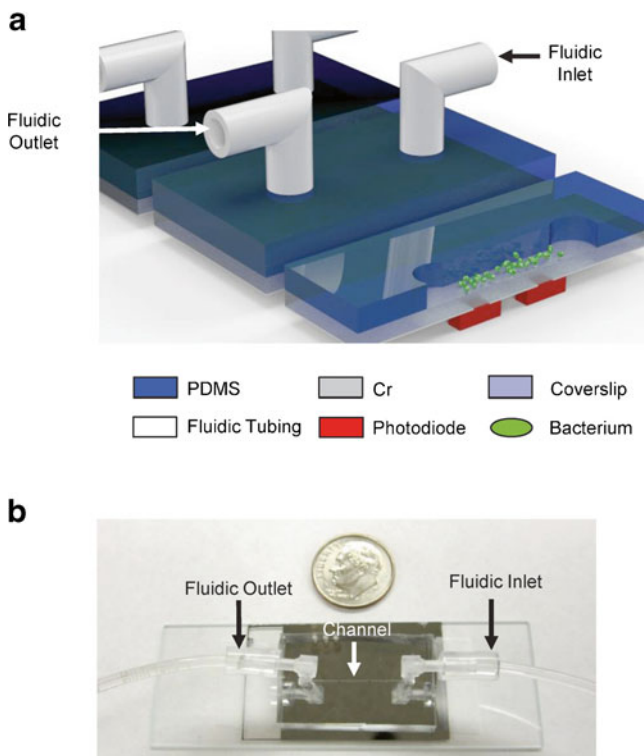
Scheme 1 a The AI-2-based circuit in *E. coli*. AI-2 (DPD) gets phosphorylated by the *E. coli* kinase LsrK. Phospho-DPD binds to the repressor LsrR derepressing the *lsr* operon and switching on the expression of related QS genes. Addition of in vitro synthesized AI-2 is known to increase biofilm formation in *E. coli* (Gonzalez Barrios et al. 2006). It has been shown that the AI-2 analog isobutyl-DPD is phosphorylated and prevents *lsr* expression through working with LsrR (Roy et al. 2010). In this study, we show that isobutyl-DPD can decrease *E. coli* biofilm formation on its own and in conjunction with antibiotics. b The QS mechanism in *P. aeruginosa* is an AI-1-based circuit where AI-1 acts through a LuxI/R homologue circuit and switches on target genes such as biofilm formation. Although *P. aeruginosa* does not synthesize any AI-2 of its own, AI-2 produced by other organisms is known to increase *P. aeruginosa* virulence (Duan et al. 2003). Ganin et al. (2009) showed that C2-alkyl analogs of AI-2 can decrease pyocyanin (a green-colored toxin) production in *P. aeruginosa*. Phenyl-DPD had a similar effect in decreasing toxin production (Gamby et al. 2012). This work demonstrates that phenyl-DPD can reduce biofilm formation in *P. aeruginosa* on its own and in conjunction with antibiotics

devices in parallel to provide simultaneous data for a control biofilm channel and for channels with biofilms undergoing different treatments. Streamlined fabrication methods also make this system compatible with integrated sensing techniques, such as electrochemical (Baldrich et al. 2011; Ben-Yoav et al. 2011), mechanical (Burg et al. 2007; Gfeller et al. 2005), and optical sensing (Renzi et al. 2005; Yacoub-George et al. 2007). Such integrated platforms, or "Lab-on-a-Chip" devices, are capable of sample analysis without reliance on external sample preparation or metrology. While not standard, we suggest microfluidic devices are ideally suited for efficient

bacterial biofilm formation, culture, and monitoring as they can be run in parallel with internal standards. Real-time optical sensing is integrated within the microfluidic biofilm detection channel, showing the gradual appearance and clearance of the biofilms continuously over time in response to various treatments. In this way, experiments are not restricted to single end point measurements.

In addition to observing the effects of isobutyl-DPD and phenyl-DPD on *E. coli* and *P. aeruginosa* biofilm growth, we observe clearance of preformed biofilms. Leveraging the enhanced flexibility provided by the microdevices, we

**a**

Fluidic Outlet

Fluidic Inlet

PDMS   Cr   Coverslip

Fluidic Tubing   Photodiode   Bacterium

**b**

Fluidic Outlet    Channel    Fluidic Inlet

**Fig. 1** **a** Schematic and **b** photograph of the microfluidic flow cell in which biofilms were formed. The width, length, and height of the straight microfluidic channel used in these studies were 500 μm, 2 cm, and 100 μm, respectively. A syringe pump was operating in withdrawal mode providing flow of bacteria, growth media, or fluorescent dye from a reservoir through the channel. Several of these devices were arrayed in parallel to provide internal standards to which experimental treatments were compared

investigated if AI-2 analogs and the antibiotic gentamicin could be used to clear biofilms in a synergistic fashion. Prophylactic use of antibiotics to prevent biofilms is inadvisable, due to the risk of resistance development. Moreover, infections are most often detected once biofilms are formed; thus, the clearance of a pre-existing biofilm is clinically more relevant than prevention of biofilm formation. In this study, we show for the first time that AI-2 inhibition-based small molecule analogs can also work synergistically with antibiotics at low concentrations to clear preformed *E. coli* and *P. aeruginosa* biofilms. The universal nature of AI-2 gives access to a broad repository of bacterial biofilms to target by this antibiotic and AI-2 analog combinatorial approach.

## Materials and methods

### Microfluidic device fabrication and assembly

Fabrication of the microfluidic device (Fig. 1) was described in Meyer et al. (2011). The device base is a coverslip, which provides a transparent substrate thin enough for high-

resolution confocal microscopy. In experiments where optical density was continuously measured, coverslips were patterned with two pinholes to allow alignment of windows with embedded optics. In confocal microscopy experiments, seven fields in each channel were imaged; the coverslips were uncoated and unpatterned as optical density measurements were not performed. The microfluidic channel itself consists of polydimethylsiloxane (PDMS) molded by photo-patterned SU8-50. Here, the mold produces microfluidic channels 100 μm deep, 500 μm wide, and 2 cm long. Ports for interfacing the channel to fluidic tubing are drilled into the PDMS using a dermatological punch. The PDMS is reversibly adhered to the coverslip by soaking the bonded side of the PDMS in methanol for 1 min, then aligning and placing the section of PDMS over the coverslip. The microfluidic channel is interfaced to external fluidic components using flexible Tygon tubing and barbed tube fittings. At the fluidic outlet, one end of the tubing is connected to a syringe pump operating in withdrawal mode, and at the inlet, the other end is inserted into a sealed microcentrifuge tube (1.5 mL) serving as a reservoir for growth medium or other liquids that are flowed into the channel. Each microfluidic device is pre-sterilized using 70 % ethanol. The entire apparatus is positioned in an incubator held at 37 °C.

### Biofilm formation

The *E. coli* biofilms were formed using the strain K-12 MG1655 ATCC (47076). *P. aeruginosa* biofilms were formed using wild-type strain PAO1. For both strains, overnight cultures were diluted to an OD600 of 0.25, introduced into the microfluidic channel, and incubated with no flow at 37 °C for 2 h. Luria–Bertani (LB) growth medium was then continuously flowed into the device at a rate of 10 μL/h. As needed, this medium was supplemented with various concentrations of analog or antibiotic at specified times. In studies of biofilm inhibition, after 2 h of cell incubation, the analog diluted in LB medium is flown into the microfluidic channel for 48 h at 10 μL/h. In studies of effects on preformed biofilms, LB is introduced over the cells at 10 μL/h for a period of 36 to 48 h to yield stable biofilms. Then, the analog or analog–antibiotic combination was introduced for an additional 36 to 48 h. We ran sets of experiments in parallel using a six-device system so that day-to-day variability in biofilm formation can be minimized. That is, internal controls and experimental conditions are run in parallel so that data sets and results presented are statistically valid ($p<0.05$). We note also that time scales associated with biofilm growth in this study (on the order of days) were consistent with previous work in vitro work (Brackman et al. 2011; Geske et al. 2005; Gonzales Barrios et al. 2006; Kim et al. 2010; Shih and Huang 2002) and correlate to mouse models (Rumbaugh et al. 1999).

Biofilm staining and confocal microscopy

Biofilms were stained in situ for microscopy. They were first treated with a Live/Dead bacterial labeling kit (Invitrogen #L7012) in which two labeling components were mixed in a 1:1 ratio to a final volume of 10 μL. The dye was introduced into the channel at 10 μL/h, the same flow rate as during biofilm growth, but for 1 h. This treatment was then followed by 10 μL/h of a 100-μg/mL solution of calcofluor (Fluorescence Brightener 28, Sigma #F3543), which binds to beta-linked polysaccharides contained in the biofilm matrix (Hamon and Lazazzera 2001; Shih and Huang 2002; Stewart et al. 1995), again for 1 h. The dyes are fixed by flowing in 3 % paraformaldehyde at the same flow rate. The staining methods were kept constant for both strains of bacteria.

Labeled samples are imaged using a confocal microscope (Zeiss LSM710). For unpatterned coverslips, Z-stacks were obtained at seven points in each microfluidic channel, and each stack was comprised of 150 slices. For patterned coverslips used while measuring the optical density of the biofilms, two stacks were obtained in each channel (i.e., one at each pinhole). The image stacks were analyzed using COMSTAT (Heydorn et al. 2000), which provides morphological characteristics. Average biofilm thickness and biomass were averaged over the image stacks obtained at each of these seven data points in the microfluidic channel. Additionally, surface reconstructions of the biofilms were created using Imaris (Bitplane) to aid in visualization of the resulting structures. Images displayed were selected from locations where the thickness and biomass were closest to the average of all measurements.

## Results

Biofilm maturation in the presence of AI-2 analog

The effect of the analog on biofilm growth was tested by continuously exposing cells to analog diluted in LB. Two concentrations of analog were investigated; the lower concentration, 40 μM, was selected based on a previous work (Roy et al. 2010), whereas the higher concentration, 100 μM, was empirically selected as a representative value at which biofilms were significantly reduced (not shown). In Fig. 2a, perfusion of LB media enabled E. coli biofilm growth to an average thickness of 19 μm and an average biomass of 14 μm³/μm² by the end of the incubation period (48 h). The presence of 40 μM isobutyl-DPD inhibited the biofilm growth by ~70 %, yielding 7-μm-thick films with a biomass of 3.5 μm³/μm². Increasing analog concentration to 100 μM had no further inhibitory effect on biofilm thickness. Surface rendering images of the biofilms confirmed that without isobutyl-DPD, the biofilm was much thicker
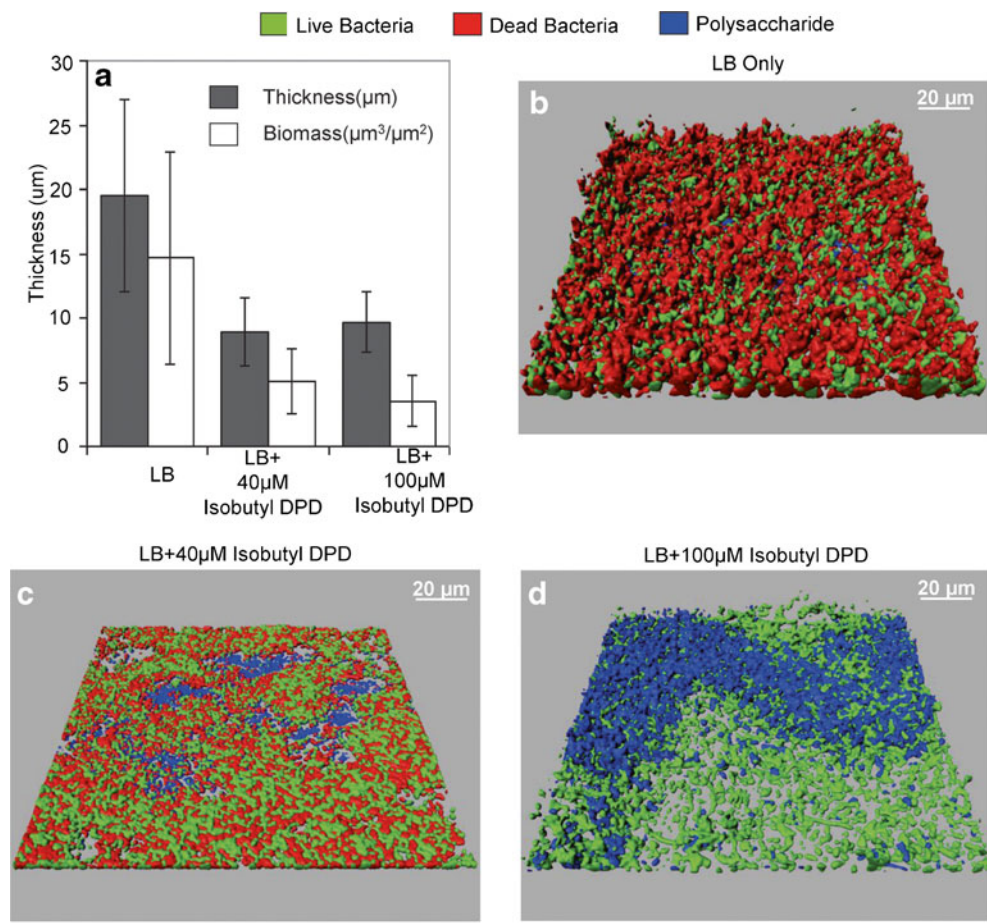
and more structured; morphological features of these biofilms include more void space, microchanneling, and larger groupings of live and dead cells (Fig. 2b). The presence of either concentration of analog investigated yielded biofilms more like thin bacterial carpets (Fig. 2c, d). A striking difference, however, was found between the isobutyl-DPD-treated cultures. The biofilm with 100 μM isobutyl-DPD appeared sparser and with less surface coverage than that exposed to 40 μM isobutyl-DPD. Interestingly, after applying the BacLight Live/Dead assay solutions under flow conditions for an hour, we found qualitatively that the biofilm was virtually free of nonviable cells and a preponderance of polysaccharide was found for the 100-μM isobutyl-DPD case. Because we have not provided a device-specific calibration of this assay, we include our qualitative results to provide insight on the relative abundance of live and dead cells only. We provide a rationale for these observations in the "Discussion" section. These results are first to demonstrate that AI-2 analog, isobutyl-DPD, a known inhibitor of QS responses that acts by repressing the lsr operon (Roy et al. 2010), can decrease biofilm formation in E. coli.

Effects of analog on preformed E. coli and P. aeruginosa biofilms

These phenotypic changes spurred our interest in testing whether the analog could alter existing biofilms. Did the presence of the AI-2 analog influence the "binding" capability of bacteria? Did the analog promote production of polysaccharide in film? As isobutyl-DPD is an established QS quencher, it is neither bacteriostatic nor bacteriocidal among planktonic cells (Roy et al. 2010). Thus, if isobutyl-DPD were used to treat the bacteria and the pathogenic bacterial populations were not removed from the host, an infection would persist. While our live biofilms seemed to persist, owing to their apparent thinner and more porous structure, we hypothesized that antibiotic co-administration could be more effective in their eventual eradication.

In order to test this approach, combinations of gentamicin (5 μg/mL) with increasing concentrations of isobutyl-DPD (40 and 100 μM) were used to treat pre-established E. coli biofilms. The control biofilm, exposed to LB medium only, exhibited an average thickness of 12 μm and an average biomass of 8.5 μm³/μm² (Fig. 3a). Addition of gentamicin without AI-2 analog decreased the thickness slightly to 10 μm, yet the biomass dropped by ~50 % (3.5 μm³/μm²). However, addition of a cocktail of antibiotic and analog (40 μM isobutyl-DPD) decreased the average biofilm thickness to 6 μm (Fig. 3a). Most importantly, this study showed that 100 μM isobutyl-DPD used with gentamicin was the most effective in clearing the preformed biofilm, shown by the reduction in thickness by more than 80 % to an average

**Fig. 2** Analysis of *E. coli* biofilm thickness and architecture in response to isobutyl-DPD. **a** Thickness and biomass of biofilm analyzed by COMSTAT (average of four different points). **b–d** Representative Imaris 3D surface reconstructions of the biofilm with **b** LB only, **c** LB+ 40 μM isobutyl-DPD, **d** LB+ 100 μM isobutyl-DPD. Images were selected from locations with average thicknesses and biomasses closest to the average of all points analyzed

Live Bacteria    Dead Bacteria    Polysaccharide

LB Only

Thickness(μm)
Biomass($\mu m^3/\mu m^2$)

LB    LB+ 40μM Isobutyl DPD    LB+ 100μM Isobutyl DPD

LB+40μM Isobutyl DPD      LB+100μM Isobutyl DPD

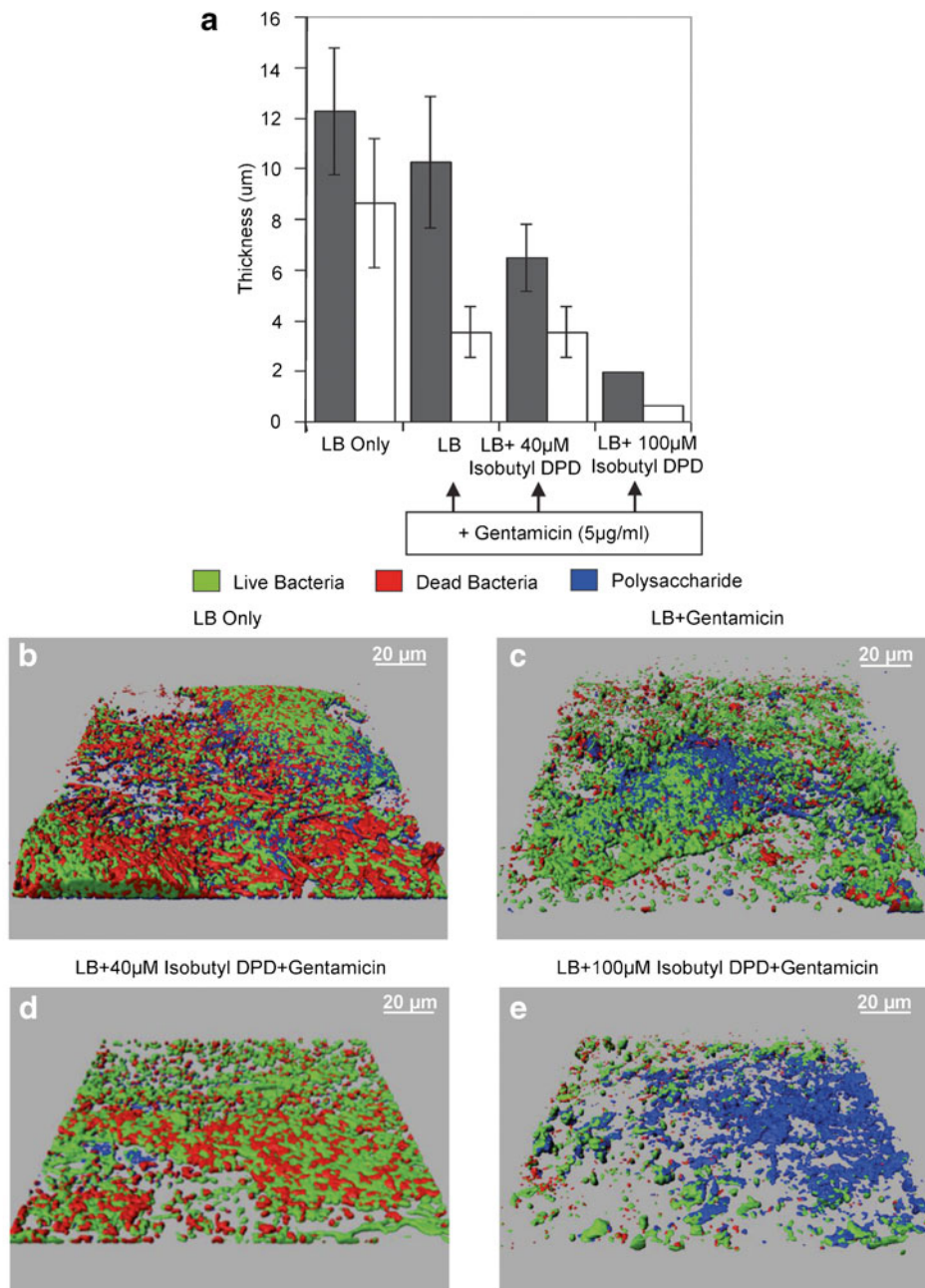Note : - Analog was flown in continuously while the biofilm formed for 48hours.

of 2 μm and by the near complete removal of biomass. The 3D surface rendering images confirmed morphological data (Fig. 3b–e), as the biofilm thickness and formation of 3D masses decreased significantly in the presence of both isobutyl-DPD and gentamicin.

We previously suggested mechanistic bases for these C1-alkyl analogs in *E. coli* (Roy et al. 2011) but had no concrete inferences of mechanisms for attenuated QS communication among otherwise AI-1 communicating *P. aeruginosa*. A recently expanded set of C1-acyl analogs of DPD revealed QS quenching activity among *P. aeruginosa* for a few cyclic compounds, phenyl-DPD in particular (Gamby et al. 2012). Here, we tested the combination of phenyl-DPD (100 μM) and gentamicin (5 μg/mL) on pre-existing *P. aeruginosa* biofilms, exactly analogous to the *E. coli* experiments. When treated with a combination of phenyl-DPD and gentamicin, *P. aeruginosa* biofilms became far thinner and sparser than untreated controls (thickness, 2 vs. 26 μm; biomass, <2 vs. 15 $\mu m^3/\mu m^2$; Fig. 4a). In addition, while gentamicin alone clears this biofilm only ~20 %, phenyl DPD can clear over~60 %, but the combination of 100 μM phenyl-DPD with 5 μg/mL of gentamicin cleared ~90 % of the biofilm thickness showing the synergistic effect between

phenyl-DPD and gentamicin in clearing preformed *P. aeruginosa* biofilms. These results were corroborated by the qualitative evaluation of the images obtained through surface rendering of confocal microscopy results (Fig. 4b–e). Biofilms grown without the addition of phenyl-DPD show denser surface coverage and mound-like structures, as opposed to the thin sheets formed by biofilms grown with phenyl-DPD. The *P. aeruginosa* biofilms treated with both phenyl-DPD and gentamicin, similar to *E. coli* results, were much sparser than controls with LB.

**Leveraging microscale biofilm reactor for streamlined measurement**

While confocal microscopy is extremely effective for characterizing bacterial biofilms, especially in conjunction with the analysis software such as COMSTAT (Heydorn et al. 2000) and Imaris, implementing this method requires extensive sample preparation and imaging time; the staining and imaging performed in this study required up to 12 additional hours, and these methods mark the end of any experiment because they terminate the sample. In addition to the benefits provided by the microliter-size channel volumes, microfluidic reactors
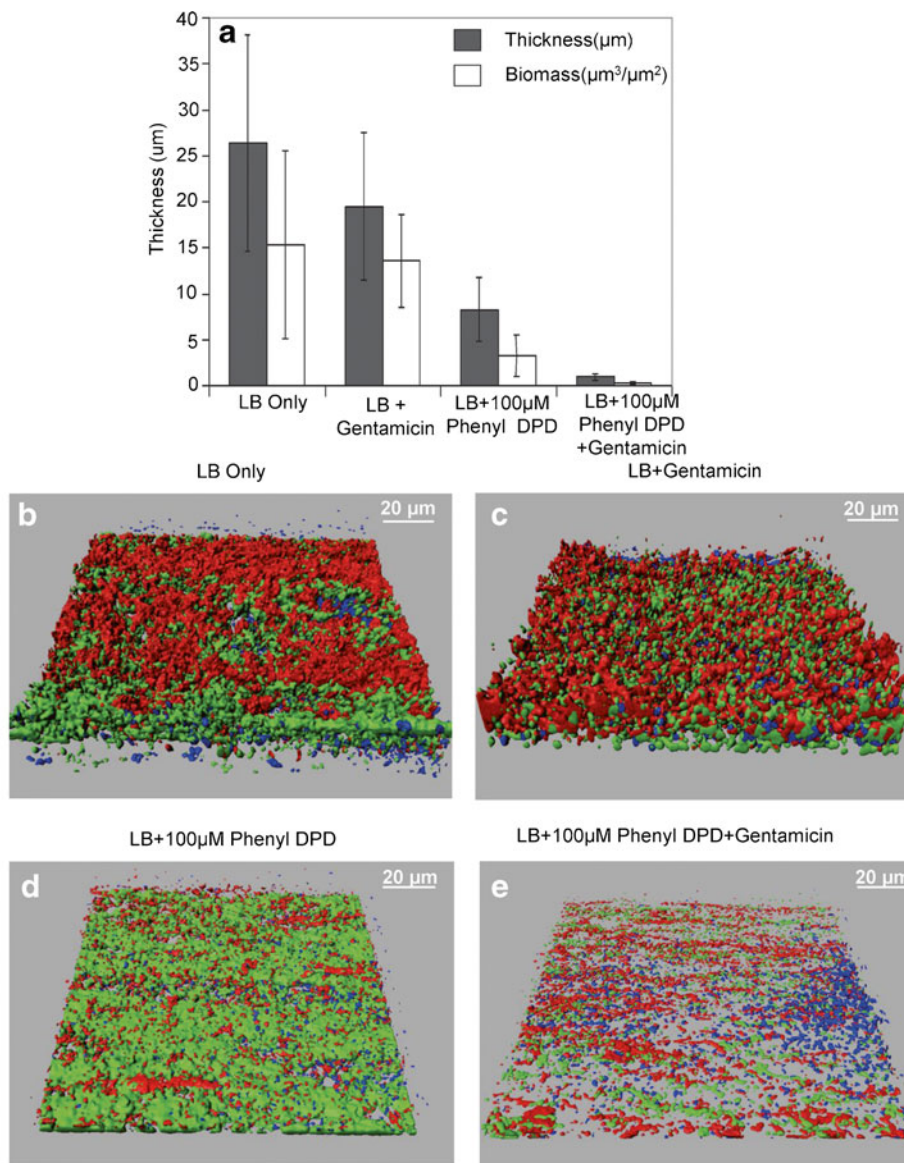
**Fig. 3** Analysis of effect of combinatorial approach analog and gentamicin on preformed *E. coli* biofilm thickness and architecture. **a** Thickness and biomass of biofilm analyzed by COMSTAT (average of five different points in the channel). **b–e** Representative Imaris 3D surface reconstructions of the biofilm with **b** LB only, **c** LB+5 μg/mL gentamicin, **d** LB+40 μM isobutyl-DPD+5 μg/mL gentamicin, **e** LB+100 μM isobutyl-DPD+5 μg/mL gentamicin. Images were selected from locations with average thicknesses and biomasses closest to the average of all points analyzed

possess the ability to integrate precise biofilm measurements with the fluidic operation of the device. In this work, the microfluidic reactor was integrated with continuous and non-invasive optical density measurement (Meyer et al. 2011) to dynamically evaluate the synergistic influence of AI-2 analog and antibiotic on preformed biofilms.

Dynamic analysis of replicate windows reveals a complex nonuniform process that, when fitted to a mathematical model, suggests relatively uniform biofilm growth overall for the first 48 h, at which time, divergent behaviors were observed based on small molecule addition (Fig. 5). For *E. coli* (Fig. 5a, b), film growth ensued unabated by the

**Fig. 4** Analysis of effect of combinatorial approach analog and gentamicin on preformed *P. aeruginosa* biofilm thickness and architecture. **a** Thickness and biomass of biofilm analyzed by COMSTAT (average of five different points in the channel). **b–e** Representative Imaris 3D surface reconstructions of the biofilm with **b** LB only, **c** LB+5 μg/mL gentamicin, **d** LB+100 μM phenyl-DPD, **e** LB+100 μM phenyl-DPD +5 μg/mL gentamicin. Images were selected from locations with average thicknesses and biomasses closest to the average of all points analyzed

addition of antibiotic as well as the combination of isobutyl-DPD and antibiotic. After 48 h, the biofilm progression deviated with the most dramatic departure being the combination of isobutyl-DPD and gentamicin. For *P. aeruginosa*, effects were roughly similar, although gentamicin alone was less effective when comparing OD and thickness (Fig. 5c, d). In all cases, however, the addition of gentamicin with QSI after 48 h slowed the progress of biofilm maturation relative to the controls, resulting in diminished films by the end of the experiments. Thus, the scenario is quite unexpected dynamically than the natural inference following experiments

depicted in Fig. 4, where one could easily hypothesize a monotonic decrease in film thickness and density upon the combined additions of phenyl-DPD and gentamicin.

While the optical data in Fig. 5a, c are presented as discrete and averaged values, in actuality, a large amount of information is gathered from the two photodiodes; by observing the temporal variance in the response (Fig. 5e), the state of the biofilm and temporal disturbances may be evaluated. It is noted that for continuous optical measurements over the two observation windows, the standard deviation in the OD values is typically less than 10 % of the

**Fig. 5** Analysis of effect of combinatorial approach on optical density and thickness using analog and gentamicin on *E. coli* (**a**, **b**) and *P. aeruginosa* (**c**, **d**) biofilms preformed for 48 h. **a** Normalized change in optical density of *E. coli* biofilms; raw data (*dotted lines*) were normalized with the change in OD at 48 h set to unity. Curves were fitted (*solid lines*) using a Churchill model (Churchill and Usagi 1972). **b** Thickness and biomass of *E. coli* biofilm analyzed by COMSTAT (average of two points in the channel). **c** Normalized change in optical density of *P. aeruginosa* biofilms; raw data (*dotted lines*) were normalized and fitted (*solid lines*) using a Churchill model. **d** Thickness and biomass of *P. aeruginosa* biofilm analyzed by COMSTAT (average of two points in the channel). **e** *Box-and-whiskers plot* of the control group (LB) in **c**, demonstrating the temporal variability observed through OD monitoring. *Each square* represents the optical data averaged between two windows and averaged over 6-h time windows centered at each point (endpoints are averaged over 3 hours). *Middle horizontal lines* represent the median, and *top and bottom horizontal lines* represent ±1 standard deviation of the data. Minimum and maximum points within the data sets are denoted by an "x"
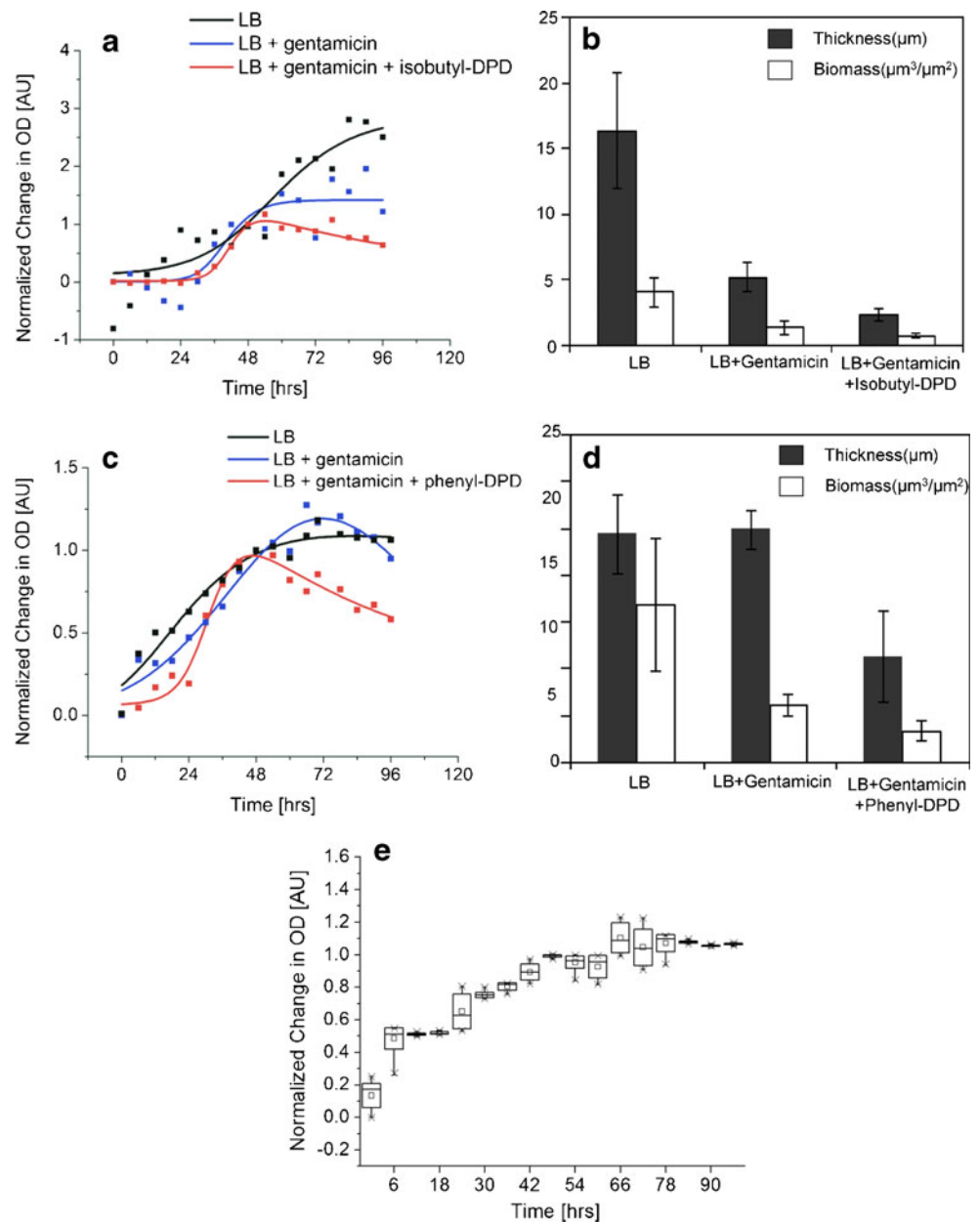


average after initial biofilm growth, as seen after the first 24 h of *P. aeruginosa* biofilm growth in the sample data in Fig. 5e. The internal consistency of the spatial and temporal variation in biofilm OD adds to the reliability of the trends in optical data observed for such a small sample volume. We note, however, that an expansion of window numbers for this and even larger biofilms would enable greater resolution of the area-based heterogeneity of the film.

## Discussion

This work demonstrates several key findings. First, biofilm development was inhibited by continuous application of C1-

alkyl AI-2 analogs. Second, combination of these analogs with sub-MIC gentamicin concentrations enables removal of preformed biofilms. Finally, the microfluidic observation platform provides critical information about short-range biofilm changes in response to treatment administration.

Compared to untreated biofilms, biofilms treated with AI-2 analogs throughout growth were thinner and less ordered as noted by an apparent lack of cohesive 3D structure, such as mounds. QS inhibitors, while not bactericidal, can mitigate biofilm formation by inhibiting bacterial communication, thereby restricting expression of genes related to biofilm formation (Davies et al. 1998; Singh et al. 2000). This suggests that the bacteria within a nascent biofilm might phenotypically be more similar to bacteria in suspension. Biofilms grown

Appl Microbiol Biotechnol (2013) 97:2627–2638

here, while continuously supplemented with AI-2 analogs, showed decreased formation even without additional antibiotic. While the AI-2 analogs did not directly kill the bacteria, interfering with the QS-regulated mechanisms involved in biofilm formation (e.g., motility—Gonzalez Barrios et al. 2006; extracellular matrix secretion—Davies et al. 1998; Nakamura et al. 2008) appeared to delay or minimize creation of stable, 3D biofilm architecture. That is, lacking the structural cohesiveness of an extracellular matrix produced with the aid of native quorum sensing (Davies et al. 1998), biofilms treated with high analog concentrations are potentially more susceptible to delamination. As nonviable cells have weaker substrate adhesion than viable cells, they are more likely to delaminate. This hypothesis is supported particularly by the results in (Fig. 2d); after growth with 100 µM isobutyl-DPD, nonviable cells were removed from the biofilm polysaccharide matrix. Conversely, the remaining polysaccharide matrix that was not able to retain these cells maintains adhesion to the substrate.

When AI-2 analog was supplemented with gentamicin, the biofilms eventually subsided, presumably because they were more susceptible to antibiotic exposure. Our study demonstrates that QS inhibitors (based on the "universal" AI-2 scaffold) are capable of dispersing and preventing biofilms on their own or potentiating the effects of traditional antibiotics for clearance of *E. coli* and *P. aeruginosa* biofilms.

The gentamicin concentration used in this study, 5 µg/mL, is on the same order of the MIC for *E. coli* K-12, 4 µg/mL (Mawer and Greenwood 1978). Also, gentamicin MIC values for *P. aeruginosa* PAO1 have been reported from 2 to 6.25 µg/mL (Kadurugamuwa et al. 1993; Kim et al. 2010). It is particularly satisfying that the effects seen here are within the normal planktonic culture-derived MIC values, which in turn, are expected to be much lower than needed for biofilms (Kim et al. 2010; Nickel et al. 1985). That is, standard inhibitory antibiotic doses for planktonic cultures are applied combinatorially with AI-2 analogs to our channels and are able to clear preformed biofilms. The potentiation of the antibiotic or anti-biofilm effects of gentamicin by co-administration with AI-2 analogs is significant because it could lead to a scenario whereby biofilms of pathogenic bacteria could be dispersed with sub-MIC levels of antibiotics, thereby preventing wanton destruction of the surrounding natural microflora. Second, the use of lower concentrations of antibiotics would retard the emergence of resistant strains. For antibiotics with a narrow therapeutic window due to toxicity to the host microflora, a strategy to lower the MIC or synergistically aid the antibiotic to clear biofilms at lower concentrations would be much welcomed.

The use of a microfluidic testing environment which used small sample volumes made this investigation possible. The integration of optical measurements in a dynamic and controllable environmental setting allowed for evaluating the

"instantaneous" state of the biofilm. This contrasts with the sole use of microscopy, which only permits an endpoint measurement. Therefore, the use of our microfluidic setup revealed phenotypic data which would have normally been lost had we only used endpoint measurements. Obtaining as much information as possible is especially important considering that the formation of a biofilm itself is highly variable. This is evidenced by the degree of variance in OD observed over time (Fig. 5e, Fig. S1). By tracking discrete points throughout biofilm growth and treatment, not only is the timescale of the contribution of the analog and antibiotic synergism toward biofilm reduction clarified, but additional information as to the instantaneous biofilm state and stability is gained. The methodology implemented here thereby promotes a more complete understanding of the temporal and spatial variance in biofilm growth.

In the translation of this work to clinical application, parameters obtained from the in vitro device that enable prediction in vivo or in other clinical situations would be valuable. The flow conditions, for example, that are imposed on biofilms within our device create shear stress levels similar to those found in interstitial fluid (Swartz and Fluery 2007). Shear stress, along with the bacterial strain, growth media, and materials used to construct the microfluidic channel, may all be adjusted to more closely mimic the environments in which biofilms typically form infections (Vertes et al. 2012). Also, owing to the microenvironments that facilitate cell–cell communication, another physical parameter, biofilm thickness, might be a good predictor of in vivo behavior. Dental biofilm thicknesses have been shown to grow to approximately 50 µm after 1 week (Al-Ahmad et al. 2007), while mature biofilms recovered from urinary catheters can range between 3 and 490 µm, depending on the formative species (Ganderton et al. 1992). A mouse model of thermal injury showed mature, 11-µm-thick *P. aeruginosa* biofilms at 46 h (Schaber et al. 2007). While the biofilms formed may be thin, the infections formed in this type of model are typically fatal within 48 h (Rumbaugh et al. 1999). Thus, the microfluidic system here yields biofilms ranging from 25 to 40 µm within 48 h that are within the appropriate ranges for extension to clinical environments. Also, the novel combinatorial treatment, as presented in this work, is ideally suited toward expanding the range of physiological, chemical, and physical parameters needed to most accurately mimic in vivo systems.

Future work, aided by new strategies for assembly and rapid removal of such biofilms within lab-on-chip devices (Cheng et al. 2011), will investigate the scope and limitations of QS inhibitor potentiation of traditional antibiotics. This work suggests the possibility of resurrecting traditional antibiotics, which were once effective but have been rendered ineffective due to bacterial resistance, by co-administration with innocuous AI-2-based QS inhibitors.

⚛ Springer

# References

Al-Ahmad A, Wunder A, Auschill TM, Follo M, Braun G, Hellwig E, Arweiler NB (2007) The in vivo dynamics of *Streptococcus* spp., *Actinomyces naeslundii*, *Fusobacterium nucleatum* and *Veillonella* spp. in dental plaque biofilm as analysed by five-colour multiplex fluorescence in situ hybridization. J Med Microbiol 56 (Pt 5):681–7. doi:10.1099/jmm.0.47094-0

Anderson GG, O'Toole GA (2008) Innate and induced resistance mechanisms of bacterial biofilms. Curr Top Microbiol Immunol 322:85–105. doi:10.1007/978-3-540-75418-3_5

Baldrich E, Munoz FX, Garcia-Aljaro C (2011) Electrochemical detection of quorum sensing signaling molecules by dual signal confirmation at microelectrode arrays. Anal Chem 83(6):2097–103. doi:10.1021/ac1028243

Ben-Yoav H, Amzel T, Biran A, Sternheim M, Belkin S, Freeman A, Shacham-Diamand Y (2011) Bacterial biofilm-based water toxicity sensor. Sensor Actuat B-Chem 158(1):366–371. doi:10.1016/j.snb.2011.06.037

Blehert DS, Palmer RJ Jr, Xavier JB, Almeida JS, Kolenbrander PE (2003) Autoinducer 2 production by *Streptococcus gordonii* DL1 and the biofilm phenotype of a luxS mutant are influenced by nutritional conditions. J Bacteriol 185(16):4851–60. doi:10.1128/JB.185.16.4851-4860.2003

Bose S, Ghosh AK (2011) Biofilms: a challenge to medical science. J Clin Diag Res 5(1):127–130

Brackman G, Cos P, Maes L, Nelis HJ, Coenye T (2011) Quorum sensing inhibitors increase the susceptibility of bacterial biofilms to antibiotics in vitro and in vivo. Antimicrob Agents Chemother 55(6):2655–61. doi:10.1128/AAC.00045-11

Burg TP, Godin M, Knudsen SM, Shen W, Carlson G, Foster JS, Babcock K, Manalis SR (2007) Weighing of biomolecules, single cells and single nanoparticles in fluid. Nature 446(7139):1066–1069. doi:10.1038/nature05741

Cheng Y, Luo X, Tsao CY, Wu HC, Betz J, Payne GF, Bentley WE, Rubloff GW (2011) Biocompatible multi-address 3D cell assembly in microfluidic devices using spatially programmable gel formation. Lab Chip 11(14):2316–8. doi:10.1039/c1lc20306a

Christensen LD, van Gennip M, Jakobsen TH, Alhede M, Hougen HP, Hoiby N, Bjarnsholt T, Givskov M (2012) Synergistic antibacterial efficacy of early combination treatment with tobramycin and quorum-sensing inhibitors against *Pseudomonas aeruginosa* in an intraperitoneal foreign-body infection mouse model. J Antimicrob Chemother 67(5):1198–206. doi:10.1093/jac/dks002

Churchill SW, Usagi R (1972) A general expression for the correlation of rates of transfer and other phenomena. AICHE J 18:1121–1128. doi:10.1002/aic.690180606

Costerton JW, Lewandowski Z, Caldwell DE, Korber DR, Lappin-Scott HM (1995) Microbial biofilms. Annu Rev Microbiol 49:711–45. doi:10.1146/annurev.mi.49.100195.003431

Costerton JW, Stewart PS, Greenberg EP (1999) Bacterial biofilms: a common cause of persistent infections. Science 284(5418):1318–22. doi:10.1126/science.284.5418.1318

Davies DG, Chakrabarty AM, Geesey GG (1993) Exopolysaccharide production in biofilms: substratum activation of alginate gene expression by *Pseudomonas aeruginosa*. Appl Environ Microbiol 59(4):1181–6. doi:0099-2240/93/041181-06

Davies DG, Parsek MR, Pearson JP, Iglewski BH, Costerton JW, Greenberg EP (1998) The involvement of cell-to-cell signals in the development of a bacterial biofilm. Science 280(5361):295–8. doi:10.1126/science.280.5361.295

de Beer D, Stoodley P, Lewandowski Z (1994) Liquid flow in heterogeneous biofilms. Biotechnol Bioeng 44(5):636–41. doi:10.1002/bit.260440510

Duan KM, Dammel C, Stein J, Rabin H, Surette MG (2003) Modulation of *Pseudomonas aeruginosa* gene expression by host microflora through interspecies communication. Mol Microbiol 50 (5):1477–1491. doi:10.1046/j.1365-2958.2003.03803.x

Dunne WM (2002) Bacterial adhesion: seen any good biofilms lately? Clin Microbiol Rev 15(2):155–166. doi:10.1128/cmr.15.2.155-166.2002

Gamby S, Roy V, Guo M, Smith JA, Wang J, Stewart JE, Wang X, Bentley WE, Sintim HO (2012) Altering the communication networks of multispecies microbial systems using a diverse toolbox of AI-2 analogues. ACS Chem Biol 7(6):1023–30. doi:10.1021/cb200524y

Ganderton L, Chawla J, Winters C, Wimpenny J, Stickler D (1992) Scanning electron microscopy of bacterial biofilms on indwelling bladder catheters. Eur J Clin Microbiol Infect Dis 11(9):789–96. doi:10.1007/bf01960877

Ganin H, Tang X, Meijler MM (2009) Inhibition of *Pseudomonas aeruginosa* quorum sensing by AI-2 analogs. Bioorg Med Chem Lett 19(14):3941–4. doi:10.1016/j.bmcl.2009.03.163

Geske GD, Wezeman RJ, Siegel AP, Blackwell HE (2005) Small molecule inhibitors of bacterial quorum sensing and biofilm formation. J Am Chem Soc 127(37):12762–3. doi:10.1021/ja0530321

Gfeller KY, Nugaeva N, Hegner M (2005) Micromechanical oscillators as rapid biosensor for the detection of active growth of *Escherichia coli*. Biosens Bioelectron 21(3):528–533. doi:DOI 10.1016/j.bios.2004.11.018

Gonzalez Barrios AF, Zuo R, Hashimoto Y, Yang L, Bentley WE, Wood TK (2006) Autoinducer 2 controls biofilm formation in *Escherichia coli* through a novel motility quorum-sensing regulator (MqsR, B3022). J Bacteriol 188(1):305–16. doi:10.1128/JB.188.1.305-316.2006

Hamon MA, Lazazzera BA (2001) The sporulation transcription factor Spo0A is required for biofilm development in *Bacillus subtilis*. Mol Microbiol 42(5):1199–1209. doi:10.1046/j.1365-2958.2001.02709.x

Herzberg M, Kaye IK, Peti W, Wood TK (2006) YdgG (TqsA) controls biofilm formation in *Escherichia coli* K-12 through autoinducer 2 transport. J Bacteriol 188(2):587–98. doi:10.1128/JB.188.2.587-598.2006

Heydorn A, Nielsen AT, Hentzer M, Sternberg C, Givskov M, Ersboll BK, Molin S (2000) Quantification of biofilm structures by the novel computer program COMSTAT. Microbiology 146(Pt 10):2395–407

Kadurugamuwa JL, Clarke AJ, Beveridge TJ (1993) Surface action of gentamicin on *Pseudomonas aeruginosa*. J Bacteriol 175 (18):5798–805. doi:0021-9193/93/185798-08

Keren I, Kaldalu N, Spoering A, Wang Y, Lewis K (2004) Persister cells and tolerance to antimicrobials. FEMS Microbiol Lett 230 (1):13–8. doi:S0378109703008565

Kim KP, Kim YG, Choi CH, Kim HE, Lee SH, Chang WS, Lee CS (2010) In situ monitoring of antibiotic susceptibility of bacterial biofilms in a microfluidic device. Lab Chip 10(23):3296–9. doi:10.1039/c0lc00154f

Kumon H, Tomochika K, Matunaga T, Ogawa M, Ohmori H (1994) A sandwich cup method for the penetration assay of antimicrobial

agents through *Pseudomonas* exopolysaccharides. Microbiol Immunol 38(8):615–9

Lewis K (2010) Persister cells. Annu Rev Microbiol 64(1):357–72. doi:10.1146/annurev.micro.112408.134306

Li J, Attila C, Wang L, Wood TK, Valdes JJ, Bentley WE (2007) Quorum sensing in *Escherichia coli* is signaled by AI-2/LsrR: effects on small RNA and biofilm architecture. J Bacteriol 189 (16):6011–20. doi:10.1128/JB.00014-07

Lowery CA, Park J, Kaufmann GF, Janda KD (2008) An unexpected switch in the modulation of AI-2-based quorum sensing discovered through synthetic 4,5-dihydroxy-2,3-pentanedione analogues. J Am Chem Soc 130(29):9200–1. doi:10.1021/ja802353j

Lowery CA, Abe T, Park J, Eubanks LM, Sawada D, Kaufmann GF, Janda KD (2009) Revisiting AI-2 quorum sensing inhibitors: direct comparison of alkyl-DPD analogues and a natural product fimbrolide. J Am Chem Soc 131(43):15584–5. doi:10.1021/ja9066783

Mah TFC, O'Toole GA (2001) Mechanisms of biofilm resistance to antimicrobial agents. Trends Microbiol 9(1):34–39. doi:10.1016/s0966-842x(00)01913-2

Mawer SL, Greenwood D (1978) Specific and nonspecific resistance to aminoglycosides in *Escherichia coli*. J Clin Pathol 31(1):12–15. doi:10.1136/jcp. 31.1.12

McNab R, Ford SK, El-Sabaeny A, Barbieri B, Cook GS, Lamont RJ (2003) LuxS-based signaling in *Streptococcus gordonii*: autoinducer 2 controls carbohydrate metabolism and biofilm formation with *Porphyromonas gingivalis*. J Bacteriol 185(1):274–84. doi:10.1128/jb.185.1.274.284.2003

Merritt J, Qi F, Goodman SD, Anderson MH, Shi W (2003) Mutation of luxS affects biofilm formation in *Streptococcus mutans*. Infect Immun 71(4):1972–9. doi:10.1128/iai.71.4.1972-1979.2003

Meyer MT, Roy V, Bentley WE, Ghodssi R (2011) Development and validation of a microfluidic reactor for biofilm monitoring via optical methods. J Micromech Microeng 21(5) doi:10.1088/0960-1317/21/5/054023

Nakamura S, Higashiyama Y, Izumikawa K, Seki M, Kakeya H, Yamamoto Y, Yanagihara K, Miyazaki Y, Mizuta Y, Kohno S (2008) The roles of the quorum-sensing system in the release of extracellular DNA, lipopolysaccharide, and membrane vesicles from *Pseudomonas aeruginosa*. Jpn J Infect Dis 61(5):375–8

Nickel JC, Ruseska I, Wright JB, Costerton JW (1985) Tobramycin resistance of *Pseudomonas aeruginosa* cells growing as a biofilm on urinary catheter material. Antimicrob Agents Chemother 27 (4):619–624. doi:10.1128/AAC.27.4.619

Olson ME, Ceri H, Morck DW, Buret AG, Read RR (2002) Biofilm bacteria: formation and comparative susceptibility to antibiotics. Can J Vet Res 66(2):86–92

Pan J, Ren D (2009) Quorum sensing inhibitors: a patent overview. Expert Opin Ther Pat 19(11):1581–601. doi:10.1517/13543770903222293

Rasmussen TB, Givskov M (2006a) Quorum-sensing inhibitors as anti-pathogenic drugs. Int J Med Microbiol 296(2–3):149–61. doi:10.1016/j.ijmm.2006.02.005

Rasmussen TB, Givskov M (2006b) Quorum sensing inhibitors: a bargain of effects. Microbiology 152(Pt 4):895–904. doi:10.1099/mic.0.28601-0

Renzi RF, Stamps J, Horn BA, Ferko S, Vandernoot VA, West JA, Crocker R, Wiedenman B, Yee D, Fruetel JA (2005) Hand-held microanalytical instrument for chip-based electrophoretic separations of proteins. Anal Chem 77(2):435–41. doi:10.1021/ac049214f

Rogers SA, Krayer M, Lindsey JS, Melander C (2009) Tandem dispersion and killing of bacteria from a biofilm. Org Biomol Chem 7(3):603–6. doi:10.1039/b817923a

Romero R, Schaudinn C, Kusanovic JP, Gorur A, Gotsch F, Webster P, Nhan-Chang CL, Erez O, Kim CJ, Espinoza J, Goncalves LF, Vaisbuch E, Mazaki-Tovi S, Hassan SS, Costerton JW (2008) Detection of a microbial biofilm in intraamniotic infection. Am J Obstet Gynecol 198(1):135e1–5. doi:10.1016/j.ajog.2007.11.026

Roy V, Smith JAI, Wang J, Stewart JE, Bentley WE, Sintim HO (2010) Synthetic analogs tailor native AI-2 signaling across bacterial species. J Am Chem Soc 132(32):11141–11150. doi:10.1021/ja102587w

Roy V, Adams BL, Bentley WE (2011) Developing next generation antimicrobials by intercepting AI-2 mediated quorum sensing. Enzyme Microb Technol 49(2):113–23. doi:10.1016/j.enzmictec.2011.06.001

Rumbaugh KP, Griswold JA, Iglewski BH, Hamood AN (1999) Contribution of quorum sensing to the virulence of *Pseudomonas aeruginosa* in burn wound infections. Infect Immun 67 (11):5854–5862

Schaber JA, Triffo WJ, Suh SJ, Oliver JW, Hastert MC, Griswold JA, Auer M, Hamood AN, Rumbaugh KP (2007) *Pseudomonas aeruginosa* forms biofilms in acute infection independent of cell-to-cell signaling. Infect Immun 75(8):3715–3721. doi:10.1128/iai.00586-07

Shih PC, Huang CT (2002) Effects of quorum-sensing deficiency on *Pseudomonas aeruginosa* biofilm formation and antibiotic resistance. J Antimicrob Chemother 49(2):309–14. doi:10.1093/jac/49.2.309

Singh PK, Schaefer AL, Parsek MR, Moninger TO, Welsh MJ, Greenberg EP (2000) Quorum-sensing signals indicate that cystic fibrosis lungs are infected with bacterial biofilms. Nature 407 (6805):762–4. doi:10.1038/35037627

Smith JA, Wang J, Nguyen-Mau SM, Lee V, Sintim HO (2009) Biological screening of a diverse set of AI-2 analogues in *Vibrio harveyi* suggests that receptors which are involved in synergistic agonism of AI-2 and analogues are promiscuous. Chem Commun (Camb) 45:7033–5. doi:10.1039/b909666c

Sternberg C, Tolker-Nielsen T (2006) Growing and analyzing biofilms in flow cells. Curr Protoc Microbiol Chapter 1:Unit 1B 2 doi:10.1002/9780471729259.mc01b02s00

Stewart PS, Costerton JW (2001) Antibiotic resistance of bacteria in biofilms. Lancet 358(9276):135–8. doi:S0140673601053211

Stewart PS, Murga R, Srinivasan R, Debeer D (1995) Biofilm structural heterogeneity visualized by 3 microscopic methods. Water Res 29(8):2006–2009. doi:10.1016/0043-1354(94)00339-9

Sun J, Daniel R, Wagner-Dobler I, Zeng AP (2004) Is autoinducer-2 a universal signal for interspecies communication: a comparative genomic and phylogenetic analysis of the synthesis and signal transduction pathways. BMC Evol Biol 4:36. doi:10.1186/1471-2148-4-36

Swartz MA, Fleury ME (2007) Interstitial flow and its effects in soft tissues. Ann Rev Biomed Eng 9:229–256. doi:10.1146/annure/bioeng.9.060906.151850

Vertes A, Hitchins V, Phillips KS (2012) Analytical challenges of microbial biofilms on medical devices. Anal Chem 84(9):3858–3866. doi:10.1021/ac2029997

Wen ZT, Burne RA (2004) LuxS-mediated signaling in *Streptococcus mutans* is involved in regulation of acid and oxidative stress tolerance and biofilm formation. J Bacteriol 186(9):2682–91. doi:10.1128/jb.186.9.2682.2691.2004

Yacoub-George E, Hell W, Meixner L, Wenninger F, Bock K, Lindner P, Wolf H, Kloth T, Feller KA (2007) Automated 10-channel capillary chip immunodetector for biological agents detection. Biosens Bioelectron 22(7):1368–75. doi:10.1016/j.bios.2006.06.003

Zhang TC, Bishop PL (1996) Evaluation of substrate and pH effects in a nitrifying biofilm. Water Environ Res 68(7):1107–1115. doi:10.2175/106143096x128504